Higgs boson finder and mass estimator: The Higgs boson to WW to leptons decay channel at the LHC

Vernon Barger and Peisi Huang

Phys. Rev. D **84**, 093001 — Published 7 November 2011

DOI: 10.1103/PhysRevD.84.093001

Higgs finder and mass estimator: the Higgs to WW to leptons decay channel at the LHC

Vernon Barger, Peisi Huang
Department of Physics, University of Wisconsin, Madison, WI 53706, USA

We exploit the spin and kinematic correlations in the decay of a scalar boson into a pair of real or virtual W-bosons, with both W-bosons decaying leptonically, for Higgs boson discovery at 7 TeV LHC energy with 10 fb^{-1} luminosity. Without reconstruction of the events, we obtain estimators of the higgs mass from the peak and width of the signal distribution in m_{ll}. The separation of signal and background with other distributions, such as the azimuthal angle between two W decay planes, the rapidity difference between the two leptons, missing E_T and the p_T of leptons, are also prescribed. Our approach identifies the salient higgs to dilepton signatures that allow subtraction of the continuum W*W* background.

The higgs boson is the only missing brick of the Standard Model (SM) [1]. The $h \to W^+W^- \to l\nu l\nu$ channel has been of long interest for higgs discovery[2][3][4][5][6][7], because of its relatively clean signal and the large branching fraction for m_h near $2m_W$. The CDF and DO experiments at the Tevatron and the ATLAS and CMS experiments at the LHC have searched for the $h \to W^*W^* \to \mu\overline{\nu}_\mu\nu_\mu\overline{\mu}$ process and have excluded a SM higgs in a range of m_h around 166 GeV [8][9][10][11][12]. The SM higgs production cross section times the branching fraction to two Ws in the SM is plotted in figure 1. The maximum $h \to W^*W^*$ signal from gluon fusion is at $m_h = 165$ GeV. The dominant production at $m_h < 1$ TeV occurs via the parton subprocess $gluon + gluon \to h$ and WW-fusion takes over at $m_h >$ 1 TeV[13]. Higgs production via gluon fusion could be larger than this estimate if extra colored states contribute to the gluon fusion loop [14] or it could be smaller if the weak coupling is shared by two neutral Higgs states, as would be the case in supersymmetry [15], or if the higgs has invisible decay modes.

Many phenomenological studies have been made of the $h \to W^*W^*$ signal[16][17][18][19][20] and that of the closely related $h \to Z^*Z^*$ channel [21][22][23][24][25]. The W*W* signal identification with leptonic W* decay is challenging. With two missing neutrinos, the events are not fully reconstructible. Also, the W*W* signal may have similar kinematics as the continuum W*W* background. Since the background is much larger than the signal at the LHC, differences in the distributions of the signal and background must be used to identify and quantify the Higgs signal. A typical signal event in this channel for $m_h = 160$ GeV is shown in the N(number of events) vs η (rapidity difference of the leptons) vs ϕ (azimuthal angular difference of the leptons) plot in figure 2, along with that of a sample background event, illustrating that there can be distinguishing features. Our aim is to utilize the differences in the signal and background characteristics to enable a background subtraction and make a clear identification of any higgs signal, in novel ways that have not been fully explored in other studies. Our approach relies on the SM prediction of the background distributions from the $q\overline{q} \to W^*W^*$ subprocess at NLO order[26] with the rejection of QCD jets. The theory normalization of this background can be tested in ranges of the distributions where the higgs signal of a given m_H does not contribute. Also, WZ production can serve as an independent calibration of the WW background, since the WZ final state does not have a neutral higgs signal contribution. Our focus is on the dilepton signal with missing transverse energy and no jets. Other backgrounds, such as $t\overline{t}$ and single top production, can be suppressed by jet vetoing (for the zero jet signal), and the Drell-Yan background can be suppressed by a missing transverse energy requirement [27].

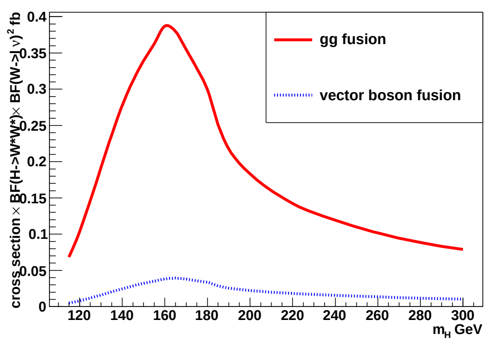

FIG. 1: SM Higgs production cross section times the branching fractions to two Ws that decay leptonically. $l = e, \mu$

Nelson [28] investigated the correlation between the two W decay planes to distinguish the higgs signal from the WW background. Choi et al[24][29] studied the signal distributions in transverse mass variables[30]. Dobrescu and Lykken [20] computed the fully differential width for higgs decays to $l\nu jj$, and constructed distributions of $m_{l\nu}$, m_{jj}, polar (θ_l) and azimuthal(ϕ_l) angles between the charged lepton in the $l\nu$ rest frame and the W^+ in the higgs rest frame, and θ_j, the angle between $-(\overrightarrow{p_l} + \overrightarrow{p_\nu})$ and the fastest jet direction in the higgs rest frame.

Estimating the higgs mass from the invariant mass of two leptons
The matrix element for the higgs signal is similar to that of muon decay, except for the placement of muon

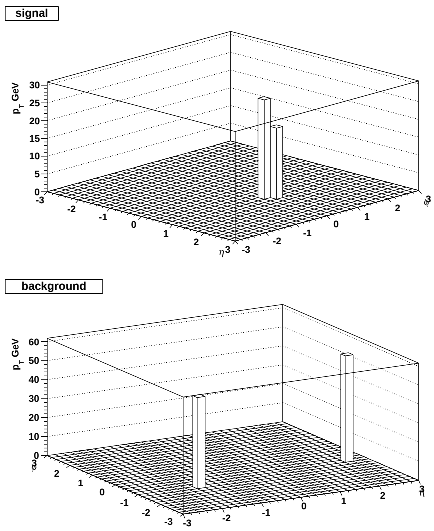

FIG. 2: Sample events for the m_h = 160 GeV signal and the W*W* background with no jets.

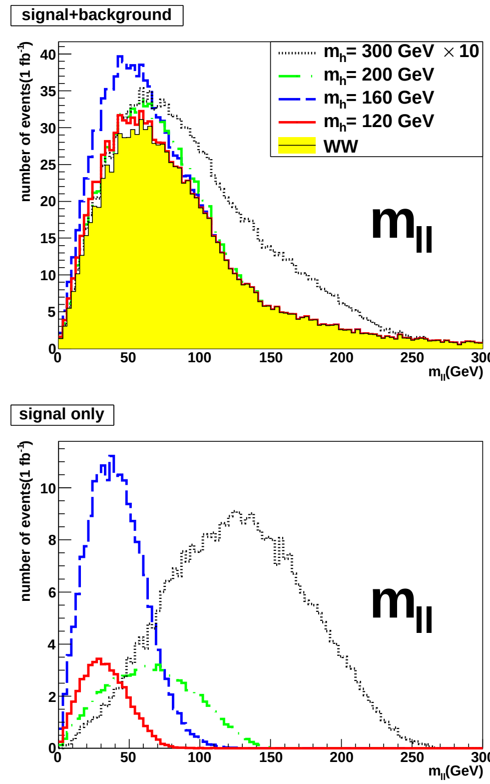

FIG. 3: m_{ll} event distribution of the SM higgs signal at various m_h and the background from continuum W*W* production for 1 fb^{-1} luminosity at 7 TeV, summed over $l = e, \mu$

.

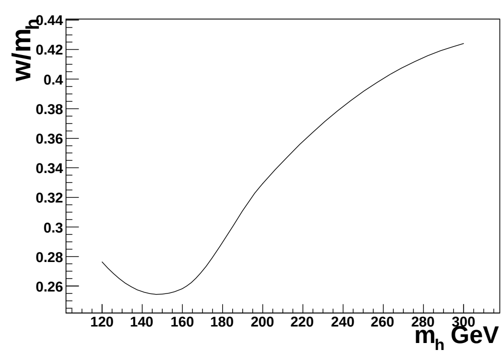

FIG. 4: Width (w) of the m_{ll} distribution of the higgs signal compare to m_h. Note that at m_h = 150 GeV(200 GeV),w = $\frac{1}{4}m_h$ (w = $\frac{1}{3}m_h$).

spinor and inclusion of off-shell W-propagators [28]. We generated 200,000 events at four different higgs mass points and W*W* background with Sherpa [31], which includes the exact tree level matrix element and QCD radiation, at 7 TeV LHC center of mass (cm) energy. Jets are defined using the anti-kt algorithm [32] with R = 0.4 and the jet clusterings are implemented using the fastjet package[33]. We use HiggsDecay [34] for calculation of the Higgs total and partial widths. We normalize the dilepton signal rate, $l = e, \mu$, for no jets to the NNLO calculation [35], which is 104 fb at m_H = 120 GeV, 389 fb at m_H = 160 GeV, 182 fb at m_H = 200 GeV, and 83 fb at m_H = 300 GeV. The $WW \to l\nu l\nu$ background is normalized to the NLO prediction [36] of 2095 fb. These cross sections are for the dilepton final states with l = e, μ, including the leptonic branching fractions. The m_{ll} distributions, with and without the WW background, are given in figure 3, each for 1 fb^{-1} integrated luminosity. The width(w) of the m_{ll} distribution is given in figure 4. This width is large compared to the total decay width of the higgs boson, making it sensitive only to the higgs mass. Here we only require two leptons and no jets, with no acceptance cuts.

The following empirical relationship between m_H and m_{ll} of the signal is found, where "peak" is the maximum and "end" is the end point of the m_{ll} distribution.

$$\begin{aligned} m_H &= 2(m_{llpeak}) + m_W \\ m_H &= m_{llend} + \frac{m_W}{2} \end{aligned} \tag{1}$$

This relationship holds for all the higgs mass points, including when one W is off-shell, near the $2m_W$ threshold and well above the threshold. The signal and W*W* background within windows around the peak values of m_{ll} are listed in Table I. In addition, we find a rather tight correlation of the Higgs mass with the width of the ll mass distribution, as discussed below.

Parametrization of the azimuthal angular distribution

The correlation function for the azimuthal angle between the two W decay planes can be parametrized as [28]:

$$F(\phi) = 1 + \alpha cos\phi + \beta cos2\phi \tag{2}$$

The direction of the normal to a W decay plane is defined as the cross product of momentum direction of the

m_h (GeV)	m_{ll} window (GeV)	signal inside window	background inside window	background outside window
120	$10-50$	373	2746	7723
160	$20-70$	1478	4326	6144
200	$30-110$	687	6713	3756
300	$60-200$	324	5901	4568

TABLE I: The signal and WW continuum background events at 7 TeV within the specified m_{ll} windows around the peak values. The number of events in the signal and background columns are for 10 fb^{-1} integrated luminosity anticipated from ATLAS and CMS combined. Event numbers are summed over $l = e, \mu$.No experimental cuts are applied here

lepton with the beam direction. In figure 5 we plot the ϕ distribution of signal and the WW background and fit the normalized distributions to Eq(2). The resulting α and β values are given in Table II.

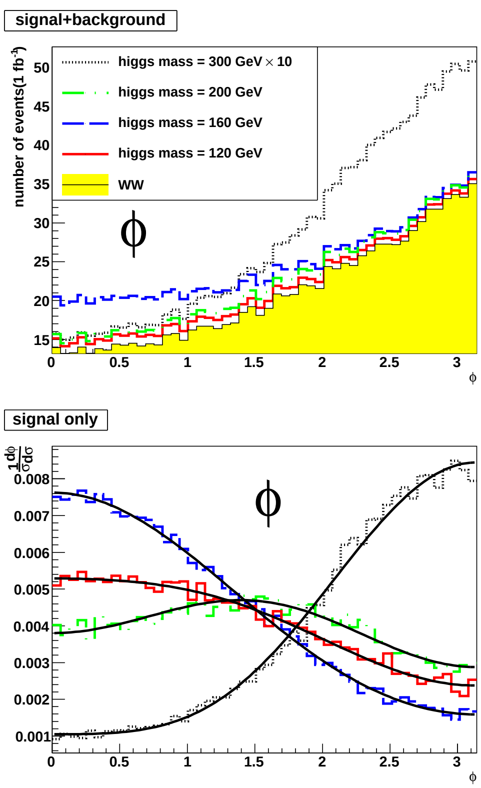

FIG. 5: The azimuthal angle between the two W decay planes, before cuts.

higgs mass (GeV)	120	160	200	300	background
α	0.36	0.68	0.12	-0.95	-0.43
β	-0.06	0.04	-0.17	0.22	0.09

TABLE II: The α and β parametrization from fit of Eq (2) to the ϕ distributions

It can be seen that $\alpha > 0$ in the transverse-transverse (TT) dominant region, while $\alpha < 0$ in the longitudinal-longitudinal (LL) dominant region. At $m_H = 1 + \sqrt{17} m_W = 182$ GeV, $\Gamma(h \to W_T W_T) = \Gamma(h \to W_L W_L)$. The ϕ distribution at $m_H = 200$ GeV is almost flat, as expected. The WW background has $\alpha < 0$, because it is LL dominant. The ϕ distributions within different m_{ll} bins are shown in Fig. 6. In the $m_{ll} < 50$ GeV bin, signal and background are both dominantly TT, and in the high m_{ll} bin, both are dominantly LL.

The pseudorapidity difference $\Delta\eta = \mid \eta_1 - \eta_2 \mid$ of the two leptons is plotted in Fig. 7. Note that the charged leptons from signal are closer in $\Delta\eta$ than for the background .

Background estimation Other variables can also differentiate signal from the background, such as $\not{E}_T = p_T(ll)$ and the p_T distribution of the fastest lepton, p_{T1}, shown in Fig. 8.

The p_T distribution of the fastest lepton is very sensitive to the higgs mass. This distribution is sharply peaked for $m_h = 160$ GeV. A recent proposed variable, ϕ^* [37] is plotted in Fig. 9. ϕ^* is defined as $\phi^* = \tan[(\pi$ - $\phi)/2]\sin\theta^*$, where ϕ is the azimuthal angle between the two leptons and $\cos\theta^* = \tanh[(\eta^- \text{-} \eta^+)/2]$, with η^- (η^+) being the pseudorapidity of the negatively charged lepton. It has been argued that ϕ^* may be more precisely determined than ϕ.

The sum of the energy of the two leptons is shown in Fig. 10. The peak value of the $E(l^+) + E(l^-)$ distribution of the signal is corelated with m_H.

Application of acceptance cuts for background rejection. Other backgrounds include $t\bar{t}$ pair production, single top production, W(or Z) + jets, the Drell-Yan process (which does not contribute to the $e\mu$ events), and $\tau\overline{\tau}$ production. All these backgrounds can be suppressed by vetoing the jets and suitable cuts on the distributions of the variables discussed above.We apply cuts following a recent ATLAS study[27].

cut 1 : no jets.
cut 2 : $m_{ll} > 15$ GeV.
cut 3 : $\text{E}_T > 30$ GeV.
cut 4 : $p_T^{ll} > 30$ GeV.
cut 5 : $\delta\phi_{ll} < 1.8$

Figure 11 shows that the shape of the m_{ll} distribution does not change under those cuts.

The ϕ distribution after experimental cuts is shown in Figure 12. The TT component is reduced by the m_{ll} cut.

The analysis of ATLAS shows that all the backgrounds except W*W* can be suppressed by cuts similar to those given above [27]. Table III shows signal and backgrounds within windows around peak value of m_{ll} after application of those cuts. Multivariable techniques, such as neural networks and boost decision trees, are another effective approach to background rejection.

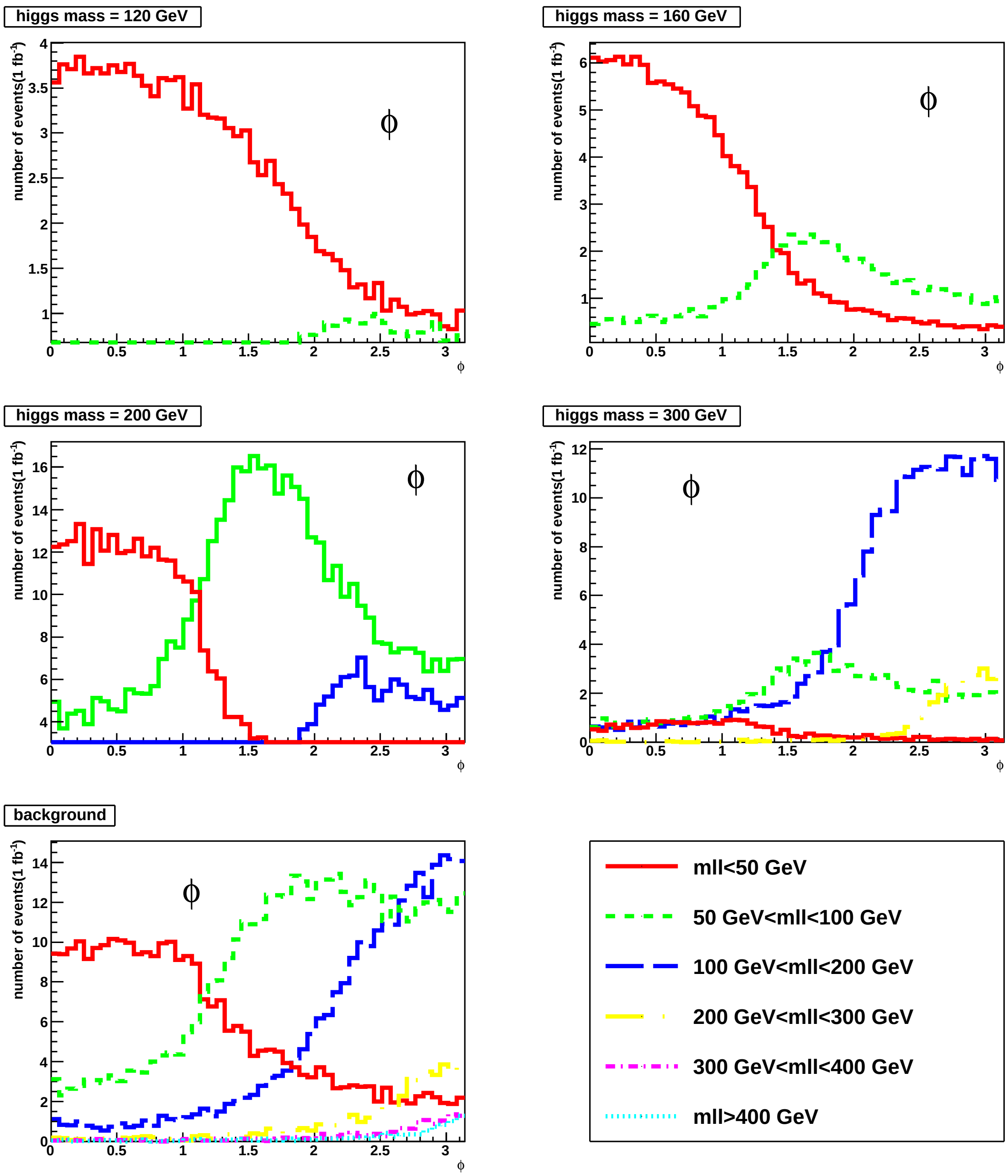

FIG. 6: ϕ distributions in different m_{ll} bins of the higgs signals and the background, before cuts.

m_h (GeV)	m_{ll} window (GeV)	signal inside window	WW inside window	$t\bar{t}$ inside window	background inside window	WW outside window	$t\bar{t}$ outside window	background outside window
120	15 – 50	45	638	151	789	743	118	861
160	20 – 70	303	899	189	1088	482	80	562
200	30 – 110	88	1022	220	1242	359	49	408
300	60 – 200	16	530	89	619	851	180	1031

TABLE III: The signal and background events at 7 TeV, after cuts, within the specified m_{ll} windows around the peak values. The number of events in the signal and background columns are for 10 fb^{-1} integrated luminosity anticipated from ATLAS and CMS combined. Event numbers are summed over $l = e, \mu$.

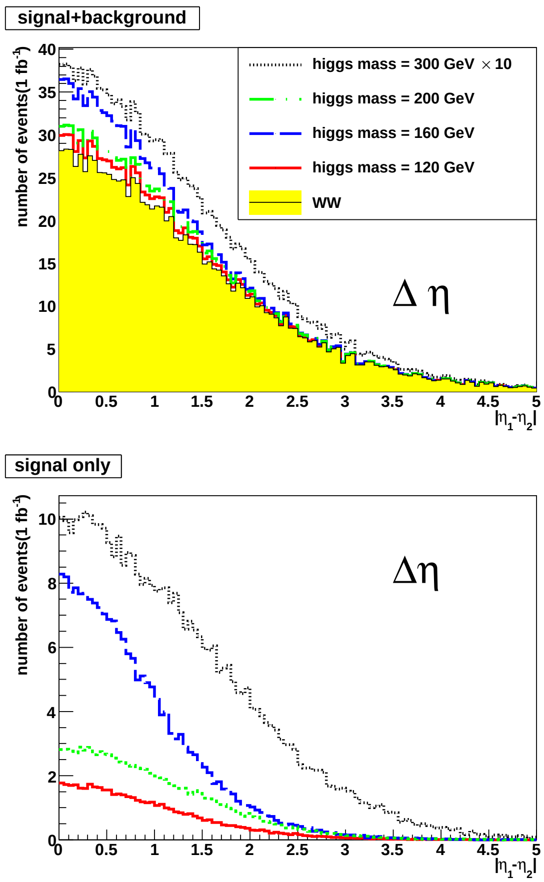

FIG. 7: Pseudorapidity difference $\Delta\eta =\mid \eta_1 - \eta_2 \mid$ of the two leptons, before cuts.

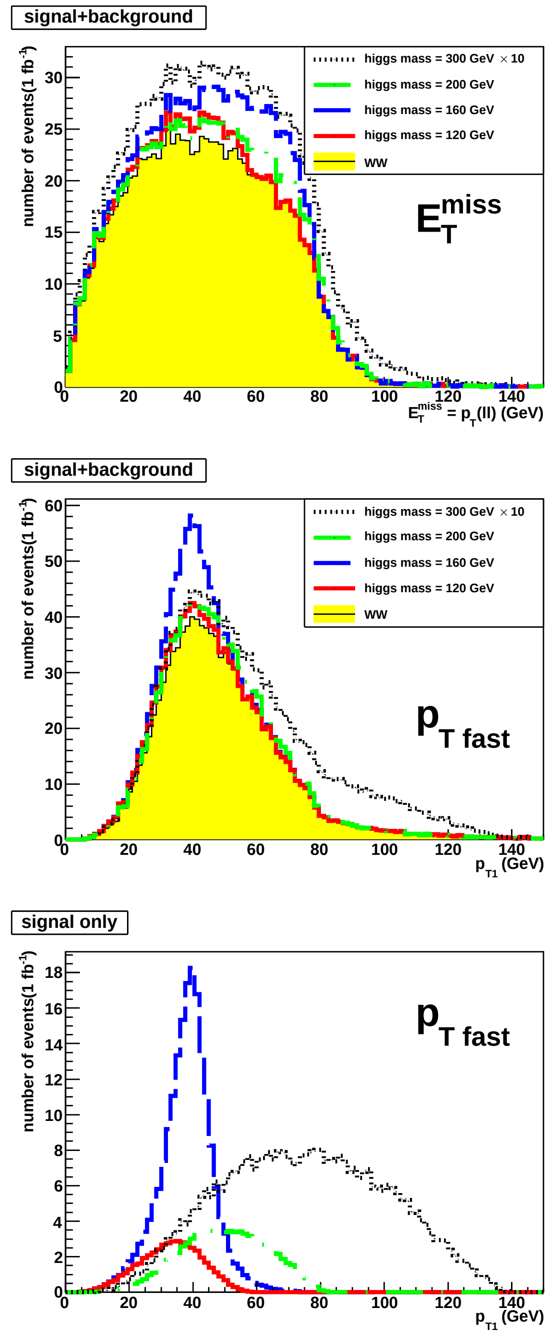

FIG. 8: The $\not{E}_T = pT(ll)$ distribution and the p_T distribution of the fastest lepton, before cuts. Note the sharply peaked p_{T1} from m_H = 160 GeV.

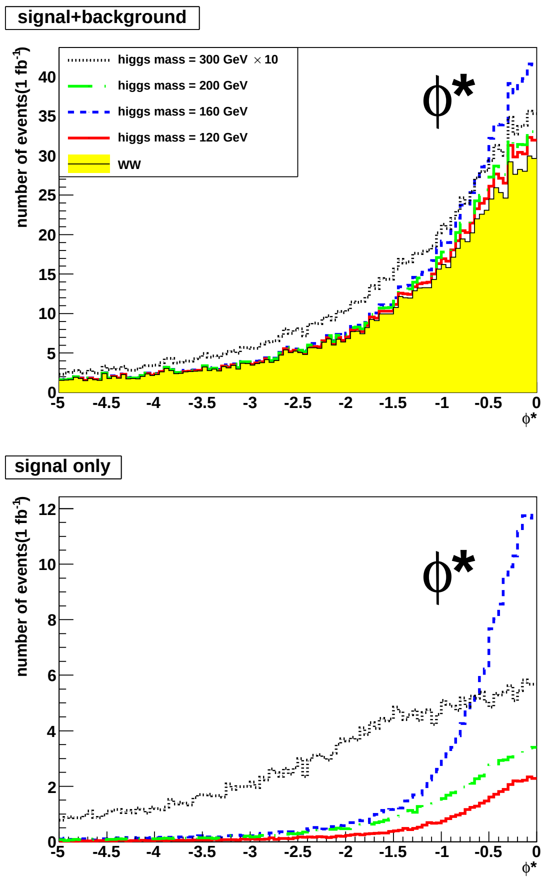

FIG. 9: ϕ * distribution, before cuts.

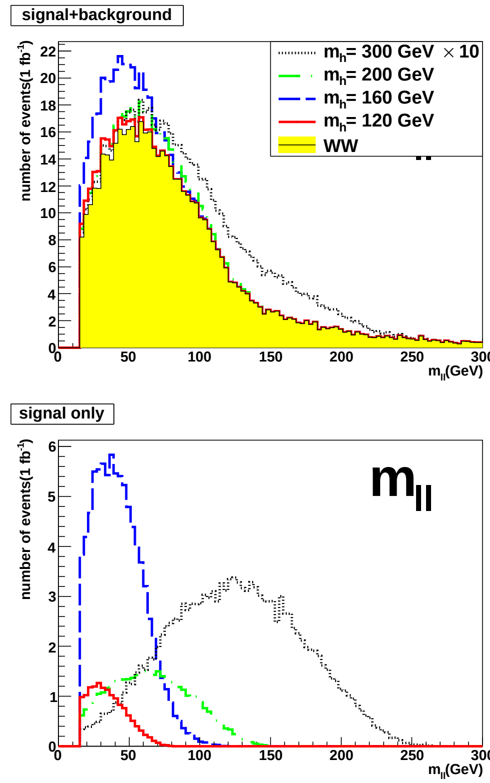

FIG. 11: m_{ll} event distribution,after cuts, of the SM higgs signal (for various m_h) and the continuum W*W* background for 1 fb^{-1} luminosity at 7 TeV, summed over $l = e, \mu$

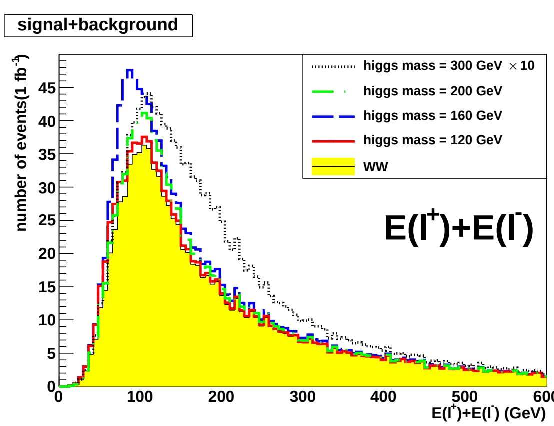

FIG. 10: Sum of energy of the two leptons, before cuts.

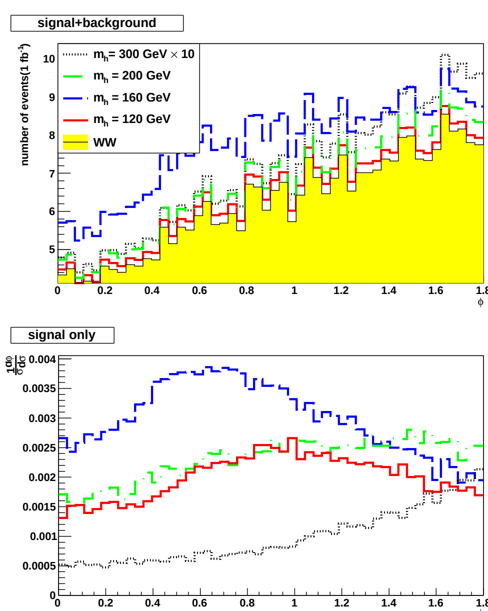

FIG. 12: The azimuthal angle between the two W decay planes, after cuts.

Conclusions and outlook After subtracting the WW continuum background from the dilepton data, the higgs mass can be estimated using Eq (1). The width of the m_{ll} distribution provides another good estimator of the higgs mass. The m_{ll}, p_T and E distributions are truncated at their lower ends by the p_T and η acceptance cuts.

Our analysis techniques can be applied to scalars in other models that decay via the WW mode such as the radion[38][39][40][41][42][43] or a dilaton [44]. The merit of the m_{ll} peak estimator in Eq(1) and width estimator in Fig.4 is their simple dependences on the higgs boson mass.

Acknowledgements This work was supported in part by the U.S. Department of Energy under grant No. DE-FG02-95ER40896.

---

[1] Abdelhak Djouadi. The Anatomy of electro-weak symmetry breaking. I: The Higgs boson in the standard model. *Phys. Rept.*, 457:1–216, 2008.

[2] Wai-Yee Keung and W. J. Marciano. Higgs-scalar decays: $H \rightarrow$ W+ X. *Phys. Rev. D*, 30(1):248–250, Jul 1984.

[3] E. W. N. Glover, J. Ohnemus, and Scott S. D. Willenbrock. Higgs-boson decay to one real and one virtual w boson. *Phys. Rev. D*, 37(11):3193–3196, Jun 1988.

[4] V. Barger, G. Bhattacharya, T. Han, and B. A. Kniehl. Intermediate-mass higgs boson at hadron supercolliders. *Phys. Rev. D*, 43(3):779–788, Feb 1991.

[5] V. Barger, Kingman Cheung, T. Han, and D. Zeppenfeld. Single-forward-jet tagging and central-jet vetoing to identify the leptonic WW decay mode of a heavy Higgs boson. *Phys. Rev. D*, 44(9):2701–2716, Nov 1991.

[6] Vernon D. Barger, King-man Cheung, Tao Han, and D. Zeppenfeld. Finding the leptonic W W decay mode of a heavy Higgs boson at hadron supercolliders. *Phys. Rev.*, D48:5433–5436, 1993.

[7] Tao Han, André S. Turcot, and Ren-Jie Zhang. Exploiting $h \rightarrow W*W*$ decays at the upgraded Fermilab Tevatron. *Phys. Rev. D*, 59(9):093001, Mar 1999.

[8] T. Aaltonen et al. Combination of Tevatron searches for the standard model Higgs boson in the W+W- decay mode. *Phys. Rev. Lett.*, 104:061802, 2010.

[9] T. Aaltonen et al. Inclusive Search for Standard Model Higgs Boson Production in the WW Decay Channel using the CDF II Detector. *Phys. Rev. Lett.*, 104:061803, 2010.

[10] Victor Mukhamedovich Abazov et al. Search for the Standard Model Higgs Boson in the H $\rightarrow$ WW $\rightarrow$lepton+neutrino+q'qbar Decay Channel. *Phys. Rev. Lett.*, 106:171802, 2011.

[11] Georges Aad et al. Limits on the production of the Standard Model Higgs Boson in pp collisions at sqrt(s) =7 TeV with the ATLAS detector. 2011.

[12] Serguei Chatrchyan et al. Measurement of WW Production and Search for the Higgs Boson in pp Collisions at sqrt(s) = 7 TeV. *Phys. Lett.*, B699:25–47, 2011.

[13] S. Dittmaier et al. Handbook of LHC Higgs Cross Sections: 1. Inclusive Observables. 2011.

[14] Qiang Li, Michael Spira, Jun Gao, and Chong Sheng Li. Higgs boson production via gluon fusion in the standard model with four generations. *Phys. Rev. D*, 83(9):094018, May 2011.

[15] Robert Harlander. Supersymmetric Higgs production at the Large Hadron Collider. *Eur. Phys. J.*, C33:s454–s456, 2004.

[16] Tao Han and Ren-Jie Zhang. Extending the higgs boson reach at the upgraded fermilab tevatron. *Phys. Rev. Lett.*, 82(1):25–28, Jan 1999.

[17] Edmond L. Berger, Qing-Hong Cao, C. B. Jackson, Tao Liu, and Gabe Shaughnessy. Higgs boson search sensitivity in the $H \rightarrow$WW dilepton decay mode at $\sqrt{s} = 7$ and 10 TeV. *Phys. Rev. D*, 82(5):053003, Sep 2010.

[18] Charalampos Anastasiou, Guenther Dissertori, Massimiliano Grazzini, Fabian Stockli, and Bryan R. Webber. Perturbative QCD effects and the search for a H $\rightarrow$WW $\rightarrow$l nu l nu signal at the Tevatron. *JHEP*, 08:099, 2009.

[19] Alan J. Barr, Ben Gripaios, and Christopher Gorham Lester. Measuring the Higgs boson mass in dileptonic W-boson decays at hadron colliders. *JHEP*, 07:072, 2009.

[20] Bogdan A. Dobrescu and Joseph D. Lykken. Semileptonic decays of the standard Higgs boson. *JHEP*, 04:083, 2010.

[21] M. J. Duncan. Higgs detection via Z^0 polarisation. *Physics Letters B*, 179(4):393 – 397, 1986.

[22] C. Zecher, T. Matsuura, and J. J. van der Bij. Leptonic signals from off-shell Z boson pairs at hadron colliders. *Z. Phys.*, C64:219–226, 1994.

[23] C. P. Buszello, I. Fleck, P. Marquard, and J. J. van der Bij. Prospective analysis of spin- and CP-sensitive variables in H $\rightarrow$ Z Z $\rightarrow$ l(1)+ l(1)- l(2)+ l(2)- at the LHC. *Eur. Phys. J.*, C32:209–219, 2004.

[24] Kiwoon Choi, Suyong Choi, Jae Sik Lee, and Chan Beom Park. Reconstructing the Higgs boson in dileptonic W decays at hadron collider. *Phys. Rev.*, D80:073010, 2009.

[25] Yanyan Gao, Andrei V. Gritsan, Zijin Guo, Kirill Melnikov, Markus Schulze, and Nhan V. Tran. Spin determination of single-produced resonances at hadron colliders. *Phys. Rev. D*, 81(7):075022, Apr 2010.

[26] J. Ohnemus. Hadronic Z Z, W- W+, and W+- Z production with QCD corrections and leptonic decays. *Phys. Rev.*, D50:1931–1945, 1994.

[27] Higgs Boson Searches using the H $\rightarrow$ WW* $\rightarrow l\nu l\nu$ Decay Mode with the ATLAS Detector at 7 TeV. Technical Report ATLAS-CONF-2011-005, CERN, Geneva, Feb 2011.

[28] Charles A. Nelson. Correlation between decay planes in Higgs-boson decays into a W pair (into a Z pair). *Phys. Rev. D*, 37(5):1220–1225, Mar 1988.

[29] Kiwoon Choi, Jae Sik Lee, and Chan Beom Park. Measuring the higgs boson mass with transverse mass variables. *Phys. Rev. D*, 82(11):113017, Dec 2010.

[30] V. Barger and R.J. Phillips. *Collider physics*. Addison-Wesley Pub. Co., Redwood City, Calif., 1987.

[31] T. Gleisberg et al. Event generation with SHERPA 1.1. *JHEP*, 02:007, 2009.

[32] Matteo Cacciari, Gavin P. Salam, and Gregory Soyez. The anti-k_t jet clustering algorithm. *JHEP*, 04:063, 2008.

[33] Matteo Cacciari and Gavin P. Salam. Dispelling the N^3 myth for the k_t jet-finder. *Phys. Lett.*, B641:57–61, 2006.

[34] A. Djouadi, J. Kalinowski, and M. Spira. HDECAY: A program for Higgs boson decays in the standard model

and its supersymmetric extension. *Comput. Phys. Commun.*, 108:56–74, 1998.

[35] Julien Baglio and Abdelhak Djouadi. Higgs production at the LHC. *JHEP*, 03:055, 2011.

[36] H Yang. Diboson Physics at the LHC. (ATL-COM-PHYS-2010-1012), Feb 2011.

[37] A. Banfi, S. Redford, M. Vesterinen, P. Waller, and T. R. Wyatt. Optimisation of variables for studying dilepton transverse momentum distributions at hadron colliders. *Eur. Phys. J.*, C71:1600, 2011.

[38] Walter D. Goldberger and Mark B. Wise. Phenomenology of a stabilized modulus. *Phys. Lett.*, B475:275–279, 2000.

[39] Kingman Cheung. Phenomenology of the radion in the randall-sundrum scenario. *Phys. Rev. D*, 63(5):056007, Feb 2001.

[40] Thomas G. Rizzo. Radion couplings to bulk fields in the Randall-Sundrum model. *JHEP*, 06:056, 2002.

[41] Graham D. Kribs. Phenomenology of extra dimensions arXiv:hep-ph/0605325. 2006.

[42] Hooman Davoudiasl, Thomas McElmurry, and Amarjit Soni. Promising Diphoton Signals of the Little Radion at Hadron Colliders. *Phys. Rev.*, D82:115028, 2010.

[43] Yochay Eshel, Seung J. Lee, Gilad Perez, and Yotam Soreq. Shining Flavor and Radion Phenomenology in Warped Extra Dimension. arXiv:1106.6218. 2011.

[44] Walter D. Goldberger, Benjamín Grinstein, and Witold Skiba. Distinguishing the higgs boson from the dilaton at the large hadron collider. *Phys. Rev. Lett.*, 100(11):111802, Mar 2008.